

**Activated dissociation of O<sub>2</sub> on Pb(111) surfaces by Pb adatoms**Yu Yang,<sup>1,2</sup> Jia Li,<sup>2</sup> Zhirong Liu,<sup>3</sup> Gang Zhou,<sup>2</sup> Jian Wu,<sup>2</sup> Wenhui Duan,<sup>2,\*</sup> Peng Jiang,<sup>4</sup> Jin-Feng Jia,<sup>2</sup> Qi-Kun Xue,<sup>2,4</sup> Bing-Lin Gu,<sup>2</sup> and S. B. Zhang<sup>5</sup><sup>1</sup>*LCP, Institute of Applied Physics and Computational Mathematics, P.O. Box 8009, Beijing 100088, People's Republic of China*<sup>2</sup>*Department of Physics, Tsinghua University, Beijing 100084, People's Republic of China*<sup>3</sup>*College of Chemistry and Molecular Engineering, Peking University, Beijing 100871, People's Republic of China*<sup>4</sup>*Institute of Physics, Chinese Academy of Sciences, Beijing 100080, People's Republic of China*<sup>5</sup>*Department of Physics, Applied Physics, and Astronomy, Rensselaer Polytechnic Institute, Troy, New York 12180, USA*

(Received 16 July 2009; published 20 August 2009)

We investigate the dissociation of O<sub>2</sub> on Pb(111) surface using first-principles calculations. It is found that in a practical high-vacuum environment, the adsorption of molecular O<sub>2</sub> takes place on clean Pb surfaces only at low temperatures such as 100 K, but the O<sub>2</sub> easily desorbs at (elevated) room temperatures. It is further found that the Pb adatoms enhance the molecular adsorption and activate the adsorbed O<sub>2</sub> to dissociate during subsequent room-temperature annealing. Our theory explains the observation of a two-step oxidation process on the Pb surfaces by the unique role of Pb adatoms.

DOI: [10.1103/PhysRevB.80.073406](https://doi.org/10.1103/PhysRevB.80.073406)

PACS number(s): 68.43.Bc, 81.65.Mq, 82.30.-b

It is of fundamental importance to understand the adsorption, dissociation, and the corresponding kinetic processes of diatomic molecules on materials surfaces.<sup>1</sup> As a prototypical example, the adsorption and dissociation of O<sub>2</sub> gas on metal surfaces have attracted considerable attention because the resulting metal oxides have been widely used as catalysts, sensors, dielectrics, and corrosion inhibitors.<sup>2</sup> In this regard, lead (Pb) (111) surface is a good model system, because atomically flat Pb(111) terraces have been fabricated on both metal and semiconductor substrates such as Ru (0001)<sup>3</sup> and Si(111).<sup>4</sup> Rich experimental and theoretical literatures are now available for such surfaces.<sup>5</sup> It was found that O<sub>2</sub> molecules adsorb on Pb(111) at temperatures as low as 100 K. Subsequent room-temperature annealing will not result in the desorption of O<sub>2</sub> but the oxidation of the Pb surface.<sup>6</sup> In contrast, the Pb(111) surface is remarkably resistant to oxidation at room temperature in the experimental environment.<sup>6,7</sup> From simple energetic argument, it is very difficult to reconcile these experimental observations, namely, how can the molecularly adsorbed O<sub>2</sub> at low temperature does not *desorb* at (elevated) room-temperature annealing, while the same O<sub>2</sub> molecules would hardly adsorb on to the same surface at the same temperature.

In this Brief Report, we explore the mechanisms for the puzzling adsorption and dissociation of O<sub>2</sub> on Pb(111) surfaces, based on first-principles total-energy calculations and thermodynamic analysis. We show that one cannot determine the state of O<sub>2</sub> at different temperatures solely from the calculated adsorption energy but rather one has to rely on the Gibbs free energy that explicitly includes the contributions from gas-phase oxygen in terms of its atomic chemical potential. Furthermore, we show that Pb adatoms, a common surface defect on epitaxial Pb terraces,<sup>8</sup> play a key role in retaining the O<sub>2</sub> adsorbed at low temperatures and assisting its dissociation once the temperature is increased. Our results are in good agreement with experiments. Importantly, such dissociation of O<sub>2</sub> molecules activated by highly mobile Pb adatoms occurs through a history-dependent process within certain thermodynamic environments. In contrast, the activation of O<sub>2</sub> dissociation by immobile defects (such as carbon

vacancy in graphite,<sup>9</sup> Pt steps on the Pt(111) surface,<sup>10</sup> and impurities on the Pb(111) surface<sup>7</sup>) are always history independent and irrelevant with thermodynamical environments such as temperature.

Our calculations are based on the density-functional theory as implemented in the Vienna *ab initio* simulation package (VASP).<sup>11</sup> The Perdew-Wang-91 (PW91)<sup>12</sup> generalized gradient approximation and the projector-augmented wave potential<sup>13</sup> are used to describe the exchange-correlation energy and the electron-ion interaction, respectively. The nudged elastic-band method<sup>14</sup> is used to find the minimum-energy path and the transition state for O<sub>2</sub> dissociation. Since the adsorption states for both molecular and atomic oxygen are nonmagnetic on the Pb(111) surface,<sup>15,16</sup> our calculations for the dissociation path of adsorbed O<sub>2</sub> are nonspin polarized. We confirm that the transition states have only one imaginary frequency. The Pb(111) surface is modeled by a 2×2 surface slab with four atomic layers and a vacuum layer of 15 Å thickness. The integration over the Brillouin zone is carried out by using the Monkhorst-Pack scheme<sup>17</sup> with a 7×7×1 grid. The cut-off energy for the plane-wave expansion is 400 eV. All the atoms, except for those at the bottom layer, are relaxed until the forces are less than 0.01 eV/Å. The calculated lattice constant for bulk Pb and the bond length for isolated O<sub>2</sub> are 5.03 and 1.24 Å, respectively, in good agreement with the experimental values of 4.95 (Ref. 18) and 1.21 Å.<sup>19</sup> To calculate the adsorption energy, we use the revised Perdew-Burke-Ernzerhof functional for the exchange-correlation energy at the already optimized geometries and the self-consistent electron densities given by PW91. This scheme is known to yield better results when compared with experiments.<sup>20</sup>

We have previously studied<sup>15</sup> in depth the molecular O<sub>2</sub> adsorption on Pb(111), which establishes the necessary initial state for the O<sub>2</sub> dissociation. Figure 1 shows the calculated dissociation path where the initial state is the molecular adsorption (MA) state and the final state is the atomic adsorption (AA) state. The MA state has no energy barrier for adsorption,<sup>15</sup> whereas the AA state is 2.29 eV lower in energy than the MA state. In the AA state, the oxygen atoms

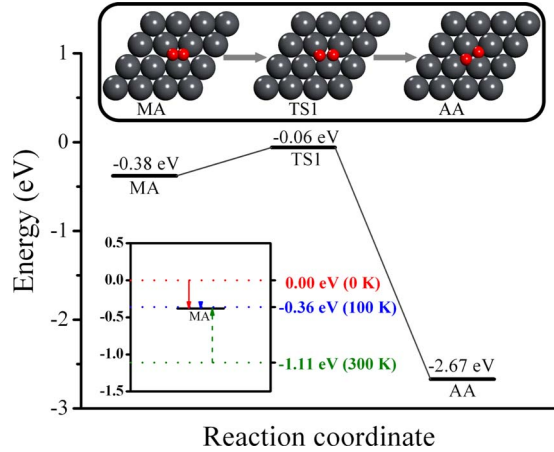


FIG. 1. (Color online).  $O_2$  energies on clean Pb (111) surface. Here, MA and AA stand for molecular and atomic adsorptions, respectively, and TS1 stands for transition state between the two. The corresponding atomic structures are given in the top panel of the figure in which gray balls are Pb and red balls are O. The lower inset shows the calculated Gibbs free energies for a free  $O_2$  at  $T=0$  (red dotted line), 100 (blue dotted line), and 300 K (green dotted line), respectively. The oxygen partial pressure in the calculation is  $2 \times 10^{-7}$  Torr.

reside at surface hollow sites, consistent with a recent calculation.<sup>16</sup> The calculated energy barrier going from MA to AA is 0.32 eV. At the transition state (TS1), the two oxygen atoms reside on two adjacent surface bridge sites separated by 1.80 Å.

Based on the van't Hoff-Arrhenius law in the harmonic approximation,<sup>21</sup> the rate coefficient  $k$  for the dissociation can be expressed as<sup>22</sup>

$$k = \frac{\prod_{i=1}^{3N} \nu_i^{MA}}{\prod_{j=1}^{3N-1} \nu_j^{TS1}} \times e^{-\Delta E/k_B T} = \nu \times e^{-\Delta E/k_B T}, \quad (1)$$

where  $\nu_i^{MA}$  and  $\nu_j^{TS1}$  are the frequencies of the eigenmodes at molecular adsorption and transition states, respectively,  $\nu$  is the attempt frequency (for  $O_2$ , the calculated  $\nu=1.33 \times 10^{13} \text{ s}^{-1}$ ),  $\Delta E$  is the energy difference between the initial and transition states, and  $k_B$ ,  $T$ , and  $N$  are the Boltzmann constant, temperature, and number of atoms, respectively. Using the barrier in Fig. 1 ( $\Delta E=0.32 \text{ eV}$ ), we obtain the rate coefficients for  $O_2$  dissociation: namely,  $\sim 10^7 \text{ s}^{-1}$  at 300 K and  $\sim 10^{-4} \text{ s}^{-1}$  at 100 K. Hence, molecular adsorption is stable at 100 K but the adsorbed  $O_2$  easily dissociates at 300 K. This conclusion, however, contradicts with experiments showing that Pb(111) surfaces are resistant to oxidation at room temperature.<sup>6,7</sup>

The origin of this discrepancy is the crucial role of thermodynamic effect in real experiments at high vacuum and variable temperature: the Gibbs free energy  $G(T, p)$ , instead of the total energy, should be used to determine the stability of the adsorption structures. In other words, we need to include the atomic chemical potential of oxygen,  $\mu_O$ . Within the ideal-gas law,  $\mu_O$  can be calculated by<sup>23,24</sup>

$$\mu_O(T, p) = \mu_O(T, p_0) + \frac{1}{2} k_B T \ln(p/p_0), \quad (2)$$

where  $p$  is the pressure and  $p_0=1 \text{ atm}$ . One can find  $\mu_O(T, p_0)$  as a function of temperature in Ref. 23: at 100 K,  $\mu_O(T, p_0)=-0.08 \text{ eV}$  and at 300 K,  $\mu_O(T, p_0)=-0.27 \text{ eV}$ . For the experimental pressure of  $p \sim 10^{-7} \text{ Torr}$ ,<sup>6,7</sup> the calculated  $\mu_O$  at 300 K is approximately  $-0.55 \text{ eV}$ . When taking into account the effect of the  $\mu_O$ , the energy of the gas-phase  $O_2$  is  $1.11-0.38=0.73 \text{ eV}$  lower than that of MA, according to Fig. 1 and its inset. In other words, molecular adsorption will not take place at room temperature. The rate coefficient at 300 K for a gas-phase  $O_2$  to dissociate with an estimated energy barrier of 1.05 eV is quite small (about  $10^{-5} \text{ s}^{-1}$ ). So neither molecular nor atomic adsorption of oxygen is likely to occur at this temperature. These results explain the observations that Pb(111) surfaces resist oxidation at room temperature.<sup>6,7</sup>

From the thermodynamic viewpoint the discrepancy at room temperature is resolved, but a new problem arises at low temperatures. According to the free energy calculation, at  $T=100 \text{ K}$  and  $p \sim 10^{-7} \text{ Torr}$ , the molecular adsorption state of  $-0.38 \text{ eV}$  is only 0.02 eV lower than that of a free  $O_2$  (as shown in the inset of Fig. 1). Therefore, at this temperature the adsorbed  $O_2$  will desorb easily. With  $\Delta E=0.32 \text{ eV}$  in Fig. 1, the rate coefficient at 100 K of  $\sim 10^{-4} \text{ s}^{-1}$  is very small. Thus the adsorbed  $O_2$  has practically no chance to dissociate to stay on the surface before it desorbs. This result, however, contradicts with the observation that  $O_2$  adsorbs on the Pb surfaces at around 100 K and oxidizes the surface upon subsequent room-temperature annealing.<sup>6</sup>

To explain the experiment, we note that surface impurities can act as nucleation centers for PbO grains from which the grains grow rapidly and autocatalytically.<sup>7</sup> Pb adatoms are commonly seen on epitaxial Pb surfaces<sup>8</sup> and readily diffuse at temperatures as low as 100 K.<sup>25</sup> Moreover, in the oxidation experiment by Ma *et al.*,<sup>6</sup> the top surfaces of all clean Pb(111) mesas are identified to be atomically flat (i.e., all mesas have flat-top geometry, but their bottom extends laterally over several atomic steps on the Si substrates), where no steps, edges, kinks, or other extended defects were observed in the oxidation region. Therefore, Pb adatoms could probably be the missing link between theory and experiment. For the adatoms to affect the oxidation, two scenarios should be considered: (i) a diffusing Pb adatom gets to the vicinity of an adsorbed  $O_2$  and the two then interact or (ii) an  $O_2$  directly adsorbs near a Pb adatom. Because the Pb adatoms are fast diffusers that very effectively transport Pb atoms from step edges to other parts of the terraces, we feel that the first scenario could be more relevant to the experiment. It is well known that the low-coordinated atoms of a metal surface have a higher activity and will speed up the reactions,<sup>26,27</sup> but such a catalytic mechanism by itself cannot explain why the oxidation on Pb surface is history dependent. However, as will be revealed below, when the effect of highly mobile defects is combined with a two-step process, the experimental puzzle can be well resolved.

To study the Pb- $O_2$  interaction, we place a Pb adatom at a

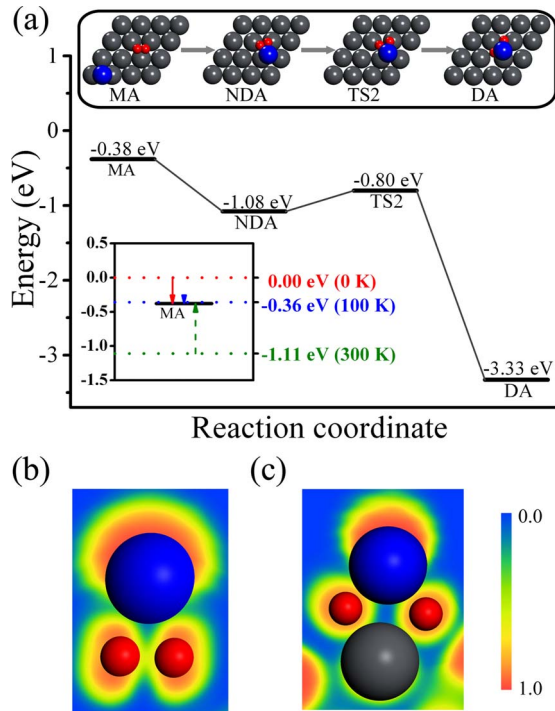


FIG. 2. (Color online). (a)  $O_2$  energies on Pb (111) surface in the presence of a Pb adatom. MA stands for the molecular  $O_2$  adsorption far away from any Pb adatom, NDA and DA stand for nondissociative and dissociative adsorptions, respectively, around the Pb adatom, and TS2 is the transition state between the two. Inset has the same meaning as the inset in Fig. 1, but for configurations shown in Fig. 2. (b) and (c) contour plots of the electron-localization function (see text) for NDA and DA, respectively, in a plane containing the Pb adatom and two oxygen atoms. Gray, blue, and red balls stand for surface Pb, Pb adatom, and O atom, respectively.

distance reasonably away from the  $O_2$  yet close enough for the two to attract each other, for example, at the second-nearest-neighbor bridge sites around the  $O_2$ . Our previous study showed that an  $O_2$  on Pb(111) has two nearly degenerate states,<sup>15</sup> and correspondingly, six different local Pb configurations. As a result of the atomic relaxation, they all converge to one of the two final states with shorter Pb- $O_2$  separations. Figure 2(a) shows the lower-energy configuration, denoted as the nondissociative adsorption (NDA) state. In the NDA state, the O-O bond length increases from 1.24 Å for isolated  $O_2$  to 1.50 Å. This suggests that the O-O bond, although not broken, is significantly weakened with a 21% elongation. The calculated O-O bond length of 1.50 Å is close to the bond length of peroxide.<sup>28</sup> Moreover, the Bader topological analysis<sup>29</sup> of the charge density shows that the two O atoms in the NDA state gain 1.85 electrons in total, also implying a peroxide state. The calculated Pb- $O_2$  binding energy is 0.70 eV, indicating that the adatoms can substantially increase the  $O_2$  adsorption.

To determine the final state of  $O_2$  dissociation in the presence of Pb adatom, we started from the NDA state and increased the distance between the two O atoms within a plane parallel to the Pb surface plane until there is no restoring force between them, and then performed structural optimization. Figure 2(a) (far right) shows the lowest-energy final state, denoted as the dissociative adsorption (DA) state. In the DA state, the distance between two O atoms is 2.94 Å, which is 137% longer than the normal O-O bond length of 1.24 Å. Electron-localization function (ELF) (Ref. 30) calculation confirms the dissociation. Figures 2(b) and 2(c) show the ELFs for the NDA and DA states. One can see clearly (weak) covalent bonding in Fig. 2(b), but not at all in Fig. 2(c). Bader topological analysis<sup>29</sup> further reveals that the two O atoms in the DA state gain 1.99 and 1.80 electrons, respectively, from the neighboring Pb atoms. The interactions between the O's and Pb in the DA state are thus ionic. A slight asymmetry in the charge transfer is because the two oxygen atoms are on inequivalent surface sites.

Figure 2(a) shows the dissociation path for  $O_2$  in the presence of Pb adatom. It can be seen that in this case, the dissociation barrier of 0.28 eV is much lower than the energy difference of 0.70 eV between the NDA and MA states. Note that at 300 K, the MA state will evolve to the desorption state (discussed earlier). Hence, an adsorbed  $O_2$  is more likely to dissociate than to desorb from the surface in this case. The calculated attempt frequency for Fig. 2 is  $\nu = 2.97 \times 10^{13} \text{ s}^{-1}$  and the corresponding rate coefficient at 300 K from NDA to the transition state TS2 is  $\sim 10^8 \text{ s}^{-1}$ . Therefore, activated by the Pb adatoms, the adsorbed  $O_2$  can easily dissociate during a room-temperature annealing. These results bring our theory into complete qualitative agreement with experiments.<sup>6,7</sup>

In summary, we have developed a comprehensive first-principles theory for the dissociation of  $O_2$  on Pb(111) surface. It is found that one needs to include oxygen atomic chemical potential given by the experimental conditions (i.e., partial pressure and ambient temperature) to qualitatively account for the observation that  $O_2$  can adsorb on clean Pb surfaces at 100 K but cannot at room temperature. In addition, Pb adatoms, commonly seen on Pb surfaces, can result in a substantial enhancement of the  $O_2$  adsorption. As a result,  $O_2$  adsorbed at low temperatures such as at 100 K is more likely to dissociate than desorbing upon subsequent room-temperature annealing. These results explain the recent puzzling experimental observations as well as demonstrating the unique role of mobile defect in activating the oxidation of lead surfaces.

This work was supported by the Ministry of Science and Technology of China (Grants No. 2006CB605105 and No. 2006CB0L0601) and the National Natural Science Foundation of China.

\*Corresponding author; dwh@phys.tsinghua.edu.cn

- <sup>1</sup>G. R. Darling and S. Holloway, Rep. Prog. Phys. **58**, 1595 (1995).
- <sup>2</sup>V. E. Henrich and P. A. Cox, *The Surface Science of Metal Oxides* (Cambridge University Press, Cambridge, 1994).
- <sup>3</sup>K. Thürmer, J. E. Reutt-Robey, E. D. Williams, M. Uwaha, A. Emundts, and H. P. Bonzel, Phys. Rev. Lett. **87**, 186102 (2001).
- <sup>4</sup>M. H. Upton, C. M. Wei, M. Y. Chou, T. Miller, and T. C. Chiang, Phys. Rev. Lett. **93**, 026802 (2004); H. Y. Lin, Y. P. Chiu, L. W. Huang, Y. W. Chen, T. Y. Fu, C. S. Chang, and T. T. Tsong, *ibid.* **94**, 136101 (2005).
- <sup>5</sup>A. Menzel, M. Kammler, E. H. Conrad, V. Yeh, M. Hupalo, and M. C. Tringides, Phys. Rev. B **67**, 165314 (2003); P. J. Feibelman, *ibid.* **62**, 17020 (2000); C. M. Wei and M. Y. Chou, *ibid.* **66**, 233408 (2002); M. Milun, P. Pervan, and D. P. Woodruff, Rep. Prog. Phys. **65**, 99 (2002).
- <sup>6</sup>X. C. Ma, P. Jiang, Y. Qi, J. F. Jia, Y. Yang, W. H. Duan, W. X. Li, X. H. Bao, S. B. Zhang, and Q. K. Xue, Proc. Natl. Acad. Sci. U.S.A. **104**, 9204 (2007).
- <sup>7</sup>K. Thürmer, E. Williams, and J. Reutt-Robey, Science **297**, 2033 (2002).
- <sup>8</sup>S. H. Chang, W. B. Su, W. B. Jian, C. S. Chang, L. J. Chen, and T. T. Tsong, Phys. Rev. B **65**, 245401 (2002); C. S. Jiang, S. C. Li, H. B. Yu, D. Eom, X. D. Wang, P. Ebert, J. F. Jia, Q. K. Xue, and C. K. Shih, Phys. Rev. Lett. **92**, 106104 (2004).
- <sup>9</sup>S. M. Lee, Y. H. Lee, Y. G. Hwang, J. R. Hahn, and H. Kang, Phys. Rev. Lett. **82**, 217 (1999).
- <sup>10</sup>P. Gambardella, Ž. Šljivančanin, B. Hammer, M. Blanc, K. Kuhnke, and K. Kern, Phys. Rev. Lett. **87**, 056103 (2001).
- <sup>11</sup>G. Kresse and J. Furthmüller, Phys. Rev. B **54**, 11169 (1996), and references therein.
- <sup>12</sup>J. P. Perdew and Y. Wang, Phys. Rev. B **45**, 13244 (1992).
- <sup>13</sup>G. Kresse and D. Joubert, Phys. Rev. B **59**, 1758 (1999).
- <sup>14</sup>G. Mills, H. Jonsson, and G. K. Schenter, Surf. Sci. **324**, 305 (1995).
- <sup>15</sup>Y. Yang, G. Zhou, J. Wu, W. H. Duan, Q. K. Xue, B. L. Gu, P. Jiang, X. C. Ma, and S. B. Zhang, J. Chem. Phys. **128**, 164705 (2008).
- <sup>16</sup>B. Sun, P. Zhang, Z. G. Wang, S. Q. Duan, X. G. Zhao, X. C. Ma, and Q. K. Xue, Phys. Rev. B **78**, 035421 (2008).
- <sup>17</sup>H. J. Monkhorst and J. D. Pack, Phys. Rev. B **13**, 5188 (1976).
- <sup>18</sup>R. W. G. Wyckoff, *Crystal Structures* (Wiley-Interscience, New York, 1965).
- <sup>19</sup>K. P. Huber and G. Herzberg, *Constants of Diatomic Molecules* (Van Nostrand, New York, 1979).
- <sup>20</sup>B. Hammer, L. B. Hansen, and J. K. Nørskov, Phys. Rev. B **59**, 7413 (1999) the use of the nonself-consistent electron densities introduces a negligible error due to the variational principle.
- <sup>21</sup>G. H. Vineyard, J. Phys. Chem. Solids **3**, 121 (1957).
- <sup>22</sup>T. Vegge, Phys. Rev. B **70**, 035412 (2004); H. Lee, J. Li, G. Zhou, W. H. Duan, G. Kim, and J. Ihm, *ibid.* **77**, 235101 (2008).
- <sup>23</sup>K. Reuter and M. Scheffler, Phys. Rev. B **65**, 035406 (2001).
- <sup>24</sup>Y. F. Zhao, Y. H. Kim, A. C. Dillon, M. J. Heben, and S. B. Zhang, Phys. Rev. Lett. **94**, 155504 (2005).
- <sup>25</sup>T.-L. Chan, C. Z. Wang, M. Hupalo, M. C. Tringides, and K. M. Ho, Phys. Rev. Lett. **96**, 226102 (2006).
- <sup>26</sup>B. Hammer, Phys. Rev. Lett. **83**, 3681 (1999).
- <sup>27</sup>Ž. Šljivančanin and B. Hammer, Phys. Rev. B **65**, 085414 (2002).
- <sup>28</sup>G. Geneste, J. Morillo, and F. Finocchi, J. Chem. Phys. **122**, 174707 (2005).
- <sup>29</sup>E. Sanville, S. D. Kenny, R. Smith, and G. Henkelman, J. Comput. Chem. **28**, 899 (2007).
- <sup>30</sup>ELF ranges between 0 and 1. In a structural complex, it provides a good description of the polycentric bonding as a function of the real-space coordinates. Generally speaking, a higher ELF implies a lower Pauli kinetic energy, which corresponds to having localized covalent bonds or lone electron pairs (ELF=1 would correspond to a perfect localization). For more details, see A. D. Becke and K. E. Edgecombe, J. Chem. Phys. **92**, 5397 (1990); S. Noury, F. Colonna, A. Savin, and B. Silvi, J. Mol. Struct. **450**, 59 (1998).